ARL-TR-8707 ● JUNE 2019

DEVCOM ARMY RESEARCH LABORATORY

Control Design for Articulating Turbine Rotor Blades for High-Efficiency Turbine Operation

by Sun Yi, Muthuvel Murugan, and Anindya Ghoshal

NOTICES

Disclaimers

The findings in this report are not to be construed as an official Department of the Army position unless so designated by other authorized documents.

Citation of manufacturer's or trade names does not constitute an official endorsement or approval of the use thereof.

Destroy this report when it is no longer needed. Do not return it to the originator.

ARL-TR-8707 ● JUNE 2019

Control Design for Articulating Turbine Rotor Blades for High-Efficiency Turbine Operation

by Sun Yi
North Carolina A&T State University

Muthuvel Murugan and Anindya Ghoshal
Vehicle Technology Directorate, CCDC Army Research Laboratory

REPORT DOCUMENTATION PAGE			Form Approved OMB No. 0704-0188

1. REPORT DATE *(DD-MM-YYYY)*	2. REPORT TYPE	3. DATES COVERED (From - To)
June 2019	Technical Report	1 June–31 August 2018

4. TITLE AND SUBTITLE	5a. CONTRACT NUMBER
Control Design for Articulating Turbine Rotor Blades for High-Efficiency Turbine Operation	5b. GRANT NUMBER
	5c. PROGRAM ELEMENT NUMBER

6. AUTHOR(S)	5d. PROJECT NUMBER
Sun Yi, Muthuvel Murugan, and Anindya Ghoshal	5e. TASK NUMBER
	5f. WORK UNIT NUMBER

7. PERFORMING ORGANIZATION NAME(S) AND ADDRESS(ES)	8. PERFORMING ORGANIZATION REPORT NUMBER
US Army Combat Capabilities Development Command Army Research Laboratory ATTN: FCDD-RLV-P Aberdeen Proving Ground, MD 21005	ARL-TR-8707

9. SPONSORING/MONITORING AGENCY NAME(S) AND ADDRESS(ES)	10. SPONSOR/MONITOR'S ACRONYM(S)
	11. SPONSOR/MONITOR'S REPORT NUMBER(S)

12. DISTRIBUTION/AVAILABILITY STATEMENT

Approved for public release; distribution is unlimited.

13. SUPPLEMENTARY NOTES

14. ABSTRACT

Conventional gas turbine engines are designed to operate at nearly fixed operation conditions including speed and blade geometries. If the operating conditions change, the flow incidence angles may not be optimum with the blade geometries and thus result in reduced performance. Active control of the pitch angles of compressor and turbine blades can improve performance by maintaining flow incidence angles within the optimum range for given blade geometries for varying operating conditions. Articulating the angles of turbine or compressor blade using smart material-based actuators such as Shape Memory Alloy (SMA) has been investigated under this effort. In using SMA actuators, output position tracking control plays an important role in the control process, and the control objective is to make the output position robustly follow the desired reference. A nonlinear control theory was adopted to address the hysteresis and nonlinearity. According to the system dynamics characteristics, control laws have been designed to achieve the output position tracking control and maintain the stability of the closed-loop system.

15. SUBJECT TERMS

adaptive turbomachinery blade, Shape Memory Alloy actuator, adaptive control, nonlinear control, active incident tolerant blade

16. SECURITY CLASSIFICATION OF:			17. LIMITATION OF ABSTRACT	18. NUMBER OF PAGES	19a. NAME OF RESPONSIBLE PERSON
a. REPORT	b. ABSTRACT	c. THIS PAGE			Muthuvel Murugan
Unclassified	Unclassified	Unclassified	UU	19	19b. TELEPHONE NUMBER (Include area code) (410) 278-7903

Contents

List of Figures

1. Introduction

Traditional gas turbine engines are designed to operate at nearly fixed operation conditions, including speed and blade geometries. If the operating conditions change, the flow incidence angles may not be optimum with the blade geometries and thus result in reduced performance. Active control of the pitch angles of compressor and turbine blades can improve performance by maintaining flow incidence angles within the optimum range for given blade geometries for varying operating conditions. Maintaining flow incidence angles within the optimum range can suppress the likelihood of flow separation in the blade passage and reduce the thermal stresses developed due to aerothermal loads. An adaptable articulating axial-flow compressor or turbine rotor blade can lead to a high-efficiency variable-speed gas turbine for rotorcraft or ground vehicles that may need to operate optimally at different torque/speed conditions during various maneuvers. Articulating the angles of turbine or compressor blade using smart-material-based actuators such as Shape Memory Alloy (SMA) has been investigated. SMA is a kind of active material that uses the transformation of thermal energy to mechanical energy when heated. The main advantages of SMA actuators are a high power-to-mass ratio; a clean, simpler design unlike conventional hydraulic/magnetic/electrical/electromagnetic actuators; maintainability; and silent actuation. However, they also have some shortcomings, such as slow response, parameter uncertainties, hysteresis, and nonlinearities. Hysteresis and nonlinearities are caused by the fact that SMA generates solid-to-solid phase transformation relating to temperature: martensite and austenite. Martensite, relatively soft, is the low-temperature phase, whereas austenite, the high-temperature phase, is relatively hard. In using SMA actuators, output position tracking control plays an important role in the control process, and the control objective is to make the output position robustly follow the desired reference. A nonlinear control theory is adopted to address the hysteresis and nonlinearity. According to the system dynamics characteristic, control laws are designed to achieve the output position tracking control and maintain the stability of the closed-loop system.

2. Modeling and Control

2.1 Modeling and Control Motors

The control methods for electrical DC motors and SMA are presented with simulation and experiments for illustration. The motor controllers are designed to regulate the angles of the rotor/stator blades in dynamically varying operation

conditions: proportional integral derivative (PID) controllers followed by adaptive controllers, which make the operation robust against uncertainties such as unmodeled nonlinearity and friction between fluid and blades. Two types of motors were considered: electrical DC motors and SMA actuators. SMA actuators change angular positions by electronically heating the material (possibly made of nickel [Ni]–titanium [Ti]–hafnium) and have attractive advantages such as high power-to-volume ratio. However, they have high nonlinearities such as backlash-like hysteresis and saturation. Also, an SMA actuator has a small displacement and a relatively slow response speed due to the cooling phase. These nonlinearities result in steady-state errors and limit cycle problems when conventional controllers (e.g., PID) are used for trajectory control. An electrical DC motor uses electrical power to generate rotational motions. Such motors are found widely in robots, appliances, and machines thanks to longer lifetime, lower price, and higher bandwidth. However, in general, compared with those of SMAs, the structures of DC motors are more complex due to their gears and electro drives, which require more space. Also, they are noisier and heavier. But depending on materials used, DC motors can be used at a temperature higher than a temperature at which standard NiTi alloys are used (Yi and Ulsoy 2014) (Czechowicz and Langbein 2015).

2.2 SMA Model

Typically, the SMA is modeled as

$$J\ddot{\theta} + b\dot{\theta} + k\theta + d = h\left(\theta, \dot{\theta}, u\right) + \alpha u \,, \tag{1}$$

where

- J, b, and k = effective inertia, an effective damping, and an effective stiffness, respectively
- d = unexpected disturbances
- $h(\theta, \dot{\theta}, u)$ = hysteretic nonlinear term; this term is the biggest problem and, thus, linear control approach may not work
- u = applied current
- α = input coefficient

Figure 1 shows a simple comparison of the hysteresis and nonhysteresis model with normalized temperature input and displacement output. This nonlinear property makes it difficult to apply classical control methods to SMA (Jin et al. 2015).

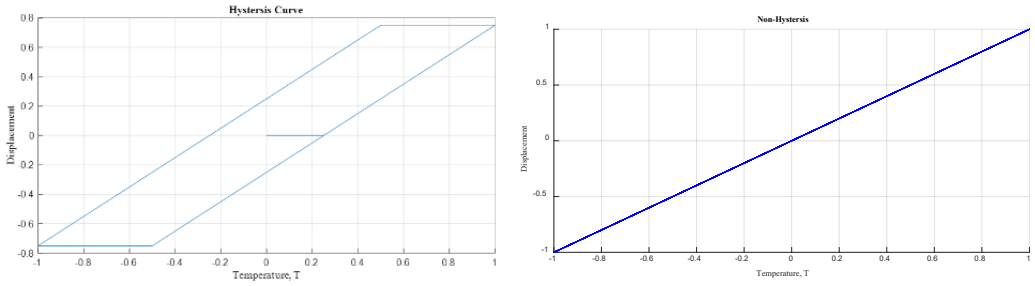

Fig. 1 Hysteresis vs. nonhysteresis

As shown in Figs. 2 and 3, when a control system designed for a nonhysteresis system is applied to a hysteresis system, it may lead to higher overshoot and more oscillations are observed. The control goal is minimizing the error $e = \theta - \theta_d$, where θ is the current angular displacement and θ_d is the desired value of blade angles. The desired values are the optimum position that yields efficient performance of the engine (Murugan et al. 2018).

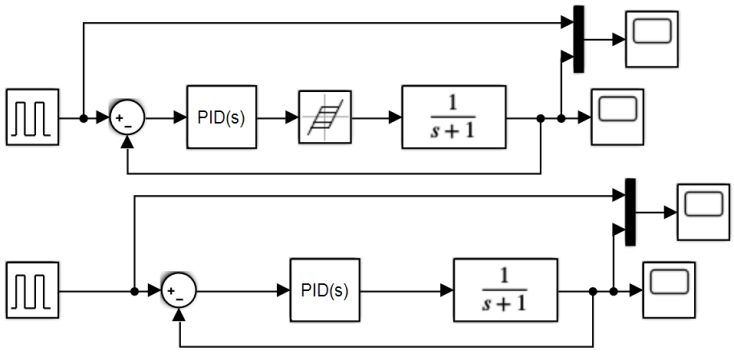

Fig. 2 Control of a system that has hysteresis: the same PID control was used for a system having hysteresis and for a normal system

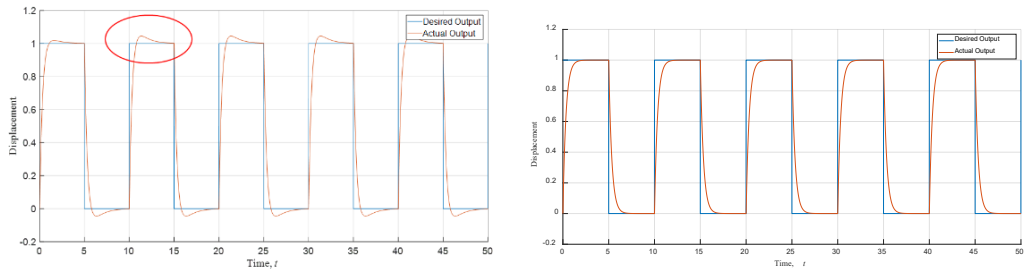

Fig. 3 Higher overshoot and more oscillations are observed (left) when the PID control designed for a nonhysteresis system (right) is applied to a hysteresis system (left)

To handle the nonlinear term in the model in Eq. 1, a nonlinear canceling method was used with delayed states (Lee and Lee 2004). This was later combined with sliding mode control to consider physical limitations in actuation (Lee et al. 2013).

In Xiaoguang et al. (2017), a nonlinear control method called feedback linearization (FBL) was used and validated through experiments. Lyapunov functions are also effective tools for nonlinear control and were used with sliding mode control in (Lechevin and Rabbath 2005).

2.3 Electric DC Motor Control

The feedback control platform for the DC motor is shown in Fig. 4. It contains the following elements:

- Electric motor (SRV-02) including a load shaft, an actuator (motor), and sensors, which are encoder and potentiometer
- Feedback controller programmed on a PC using MATLAB/Simulink and Quarc software
- Data acquisition device (QPID terminal board) made by Quanser and voltage amplifier (VolPAQ-X1)

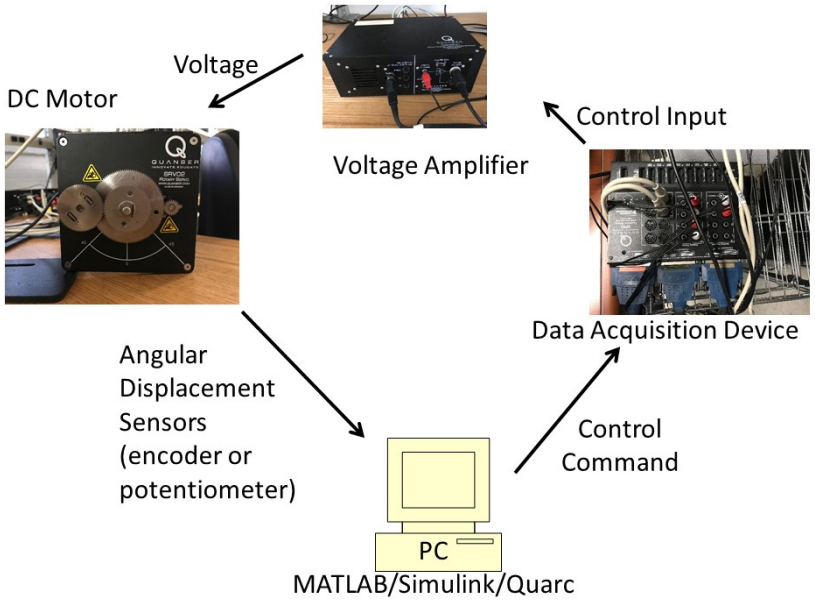

Fig. 4 Schematic of the electrical DC motor system used at North Carolina A&T State University

The voltage-to-angular position transfer function for the DC motor system (SRV-02) in Fig. 4 is given by

$$P(s) = \frac{K}{(\tau s + 1)s} = \frac{\Theta(s)}{V_m(s)} \,. \tag{2}$$

The proportional-velocity (PV) control law to follow the desired position of the motor is

$$V_m(s) = k_P\left(\theta_d - \theta\right) - k_V s\theta\,, \tag{3}$$

where k_P and k_V are the proportional and velocity control gains, respectively. The angle θ_d is the desired angle, and θ is the measured angle. Also, $V_m(s)$ is the input voltage provided by the amplifier.

When the system has the stable characteristic roots as −14.9565 ± 15.7274i, the response is as shown in Fig. 5 with the control structure in Fig. 6. The output (green) follows the desired output (blue) in Fig. 5.

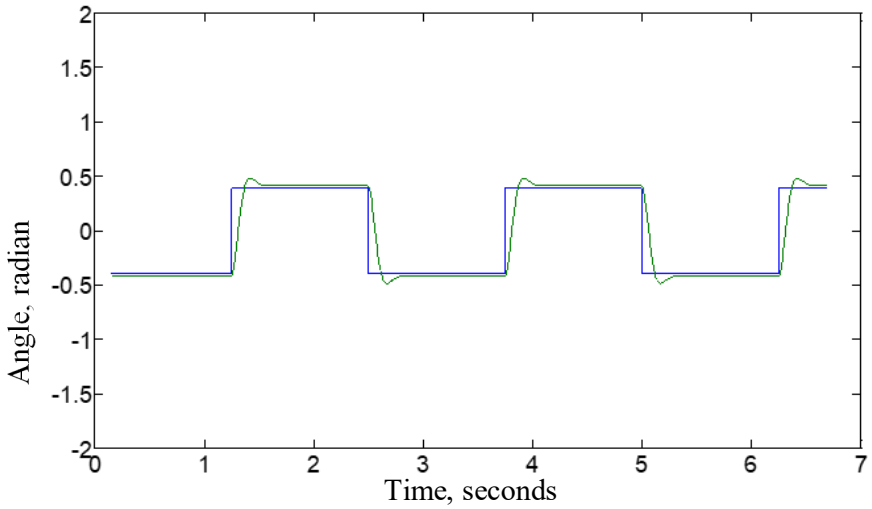

Fig. 5 Stable when PV control is used and no disturbance exists; output (green) follows the desired output (blue)

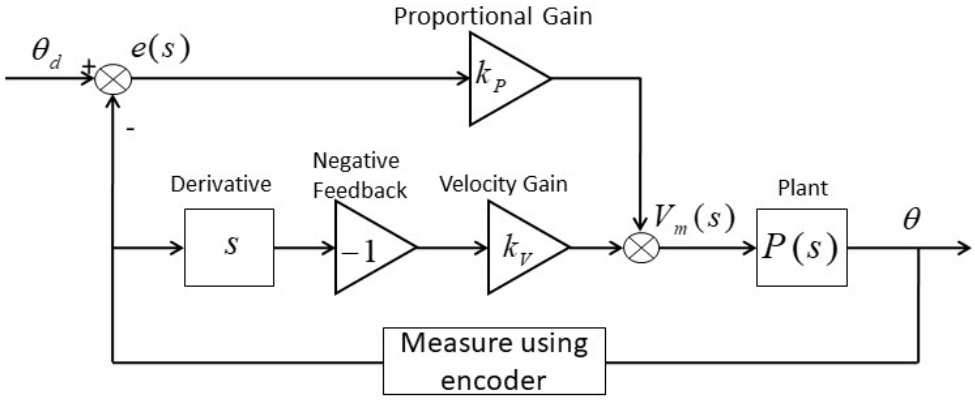

Fig. 6 Diagram for feedback control of electric DC motors

2.4 Adaptive Control for Electric Motors

As shown in Fig. 5, the controlled system shows stable performance. But if the same control was used for a system with disturbance, the response shows discrepancies between simulation and actual output. Thus a control system is needed that can modify (update in real time) its behavior in response to changes in the dynamics of the process and the disturbances. A controller with adjustable parameters and a mechanism for adjusting the parameters called the Model Reference Adaptive Control (MRAC) is used (Ioannou and Sun 1996). The output of the system is compared with a desired response from a reference model. Then the plant response matches the response of the reference model (Fig. 7). In many cases, for a given operating point the complex system dynamics are approximated by a linear time-invariant model with the given structure and constant parameters. However, when the operating condition changes, the parameters have to be changed for the appropriate approximation of system dynamics while the structure of the model usually remains unchanged. Therefore, a linear controller designed for the given operating point is unable to achieve the desired control performance at the different operating points. As shown in Fig. 1 (also in Eq. 1), the relationship between the input and the output is nonlinear. Thus a control system that can modify (update in real time) its parameters in response to changes in the dynamics of the process and the disturbances was developed. Stable performance at different conditions cannot be obtained by the fixed gain controller. So, it was necessary to introduce the adaptive control method to compensate the nonlinearity of the process.

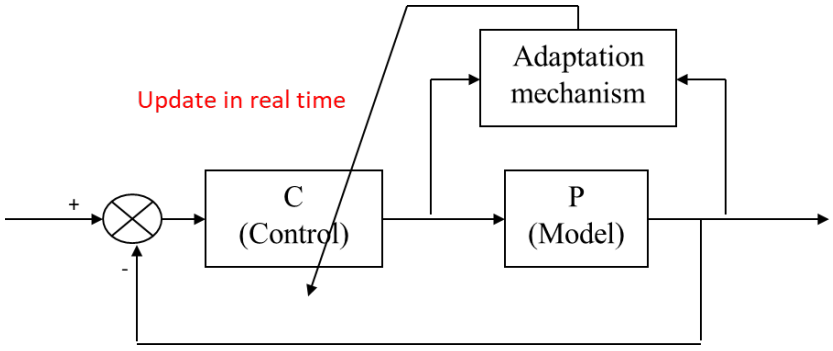

Fig. 7 Adaptive control: MRAC

A control system can modify (update in real time) its behavior in response to changes in the dynamics of the process and the disturbances. The controller has adjustable parameters and a mechanism for adjusting the parameters. In MRAC the output of the system is compared with a desired response from a reference model, thus allowing the plant's response to match the response of the reference model.

In adaptive control the controller structure consists of a feedback loop and a controller with adjustable gains. The gains of the controller are then changed so that the control performance requirements are met for different operating conditions. A feedback controller with adjustable parameters and an adaptive mechanism for adjusting the parameters is used. Model-reference adaptive control is one of the representative approaches to adaptive control. The reference model is chosen to generate the desired trajectory that the system output must follow. The tracking error, *e*, represents the deviation of the plant output from the desired trajectory. The closed-loop system is made up of an ordinary feedback control law that contains the plant and the controller and an adaptive mechanism that provide the controller parameter estimates in real time. The output of the system is compared with a desired response from a reference model. Then the plant response matches the response of the reference model.

$$V = \frac{1}{2}(e^2 + \frac{\tilde{k}^2}{\gamma})$$
$$\dot{V} = e\dot{e} + \frac{\tilde{k}\dot{\tilde{k}}}{\gamma} = -a_m e^2 - \tilde{k}ex + \frac{\tilde{k}\dot{\tilde{k}}}{\gamma} = -a_m e^2 - \tilde{k}\left(ex - \frac{\dot{\tilde{k}}}{\gamma}\right) < 0 \text{ when } \dot{k} = \dot{\tilde{k}} = \gamma ex \quad . \qquad (4)$$

This scheme was realized via the mathematic analysis summarized in Eq. 4. The Lyapunov function, V, in terms of the estimation error, e, and the parametric error, $\tilde{k}$, is set. Then its time derivative, $\dot{V}$, is negative when the adaptation rule is derived.

Figure 8 shows the motor system setup (see Fig. 4) with an asymmetrical load added to evaluate the effectiveness of the adaptive control. Comparing the responses in Figs. 9 and 10, the steady-state error in Fig. 10 is smaller and the transient response is faster because of the adaptation mechanism, as shown in Fig. 11.

Fig. 8 An asymmetrical load is added to the motor system in Fig. 4 to evaluate the effectiveness of the adaptive control as shown in Figs. 9 and 10

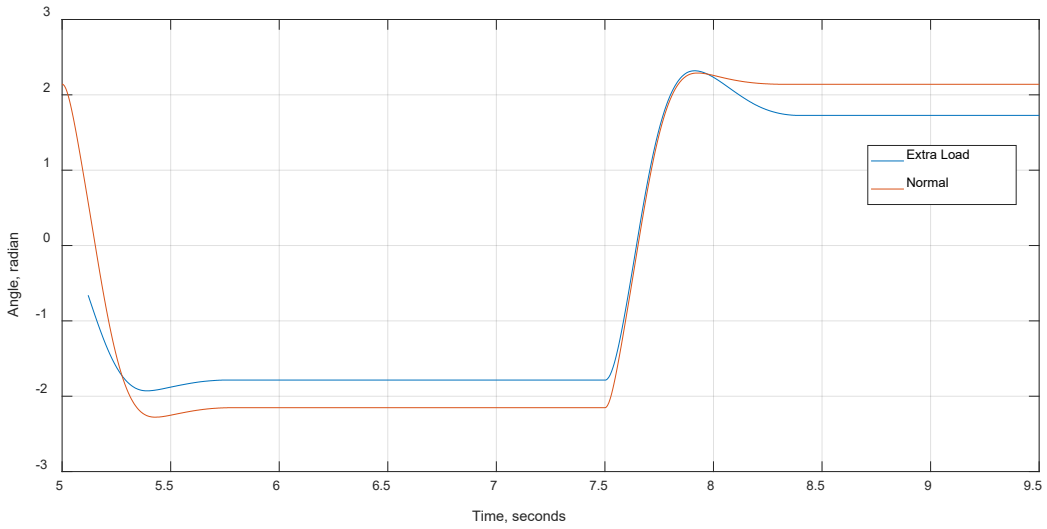

Fig. 9 Controller designed for a model was used for a system with disturbance. The responses show discrepancies between the nominal system and the system that has additional load in Fig. 8.

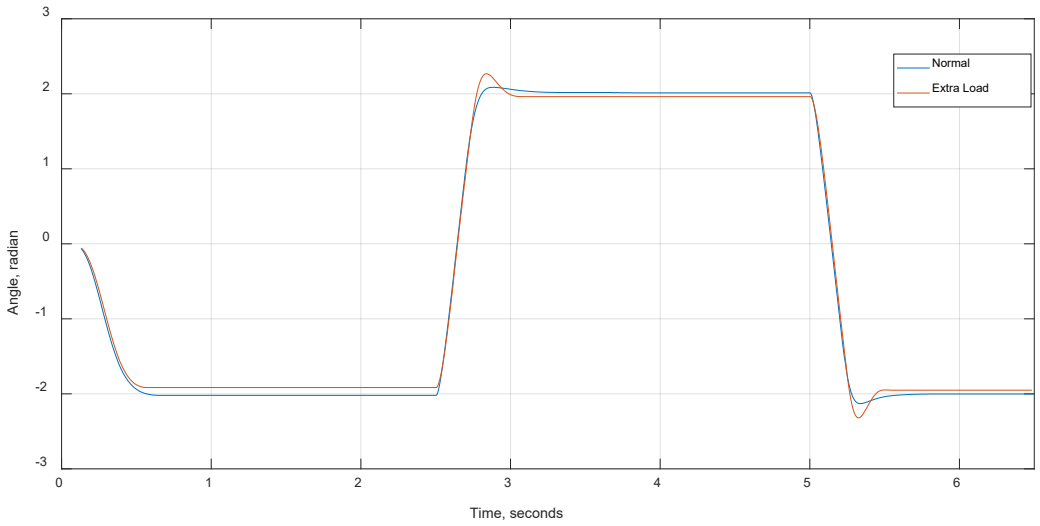

Fig. 10 Responses with MRAC. Output of the system is compared with a desired response from a reference model, thus allowing the plant response to match the response of the reference model.

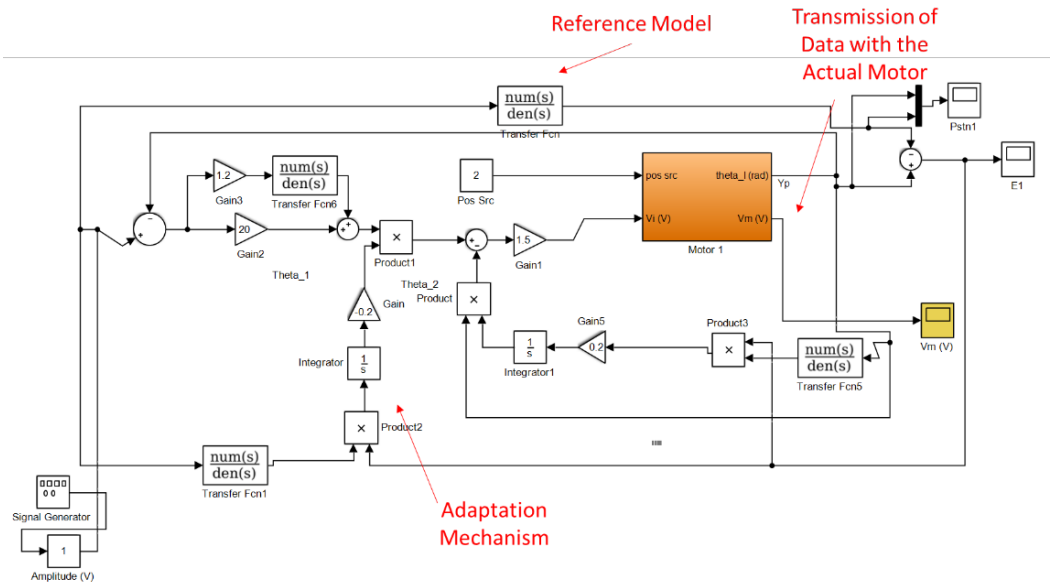

Fig. 11 MRAC for the electric DC motor

2.5 Adaptive Control for SMA

In the adaptive control, over time the error approaches zero and thus the output of the system becomes the same as the output of the reference model. This adaptation rule is implemented in Fig. 12, a block diagram of the adaptation mechanism. The reference model is chosen to be stable and have fast dynamics.

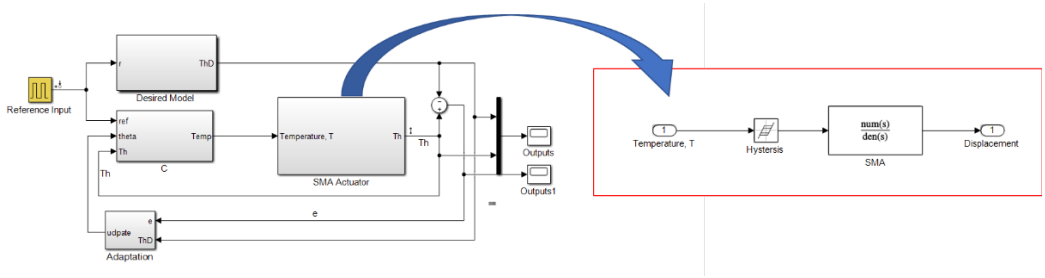

Fig. 12 MRAC for the actuator with hysteresis

For validation through simulation, the results are shown in Fig. 13. The responses in Fig. 13 show the response with adaptation is faster and with smaller steady-state errors. Using the adaptive control, it is possible to compensate for the nonlinearities in SMA and obtain improved tracking results.

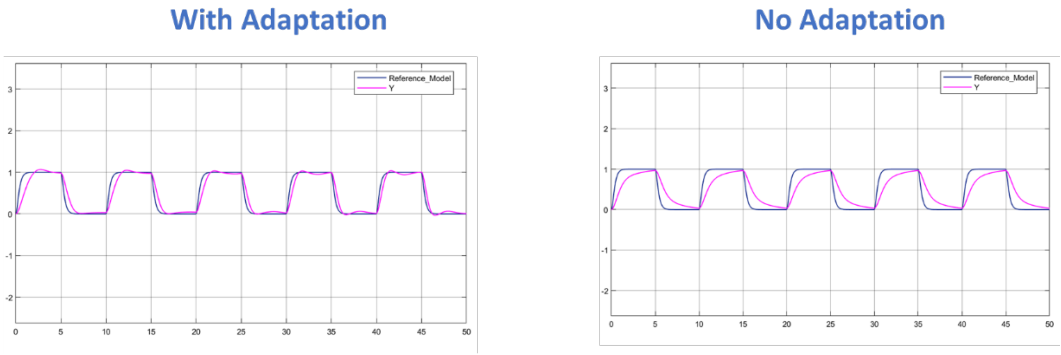

Fig. 13 Model reference adaptive control is faster and with reduced errors

3. Conclusion

Considering uncertainties and nonlinearities, the control systems that include adaptation mechanisms were developed and applied to electric DC motor and SMA actuator models. The systems with the control were simulated for illustration. Also, an experiment with the electric motor was conducted, which shows improved response in terms of steady-state errors and transient responses. The method will be applied to SMA after parameter identification and system setup.

4. References

Czechowicz A, Langbein S. Shape memory alloy valves: basics, potentials, design. Berlin (Germany): Springer; 2015.

Ioannou PA, Sun J. Robust adaptive control. Upper Saddle River (NJ): Prentice-Hall; 1996.

Jin M, Lee J, Ahn KK. Continuous nonsingular terminal sliding-mode control of shape memory alloy actuators using time delay estimation. IEEE/ASME Transactions on Mechatronics. 2015;20(2):899–909.

Lechevin N, Rabbath C. Quasipassivity-based robust nonlinear control synthesis for flap positioning using shape memory alloy micro-actuators. Proceedings of the IEEE American Control Conference; 2005.

Lee HJ, Lee JJ. Time delay control of a shape memory alloy actuator. Smart Materials and Structures. 2004;13(1):227.

Lee J, Jin M, Ahn KK. Precise tracking control of shape memory alloy actuator systems using hyperbolic tangential sliding mode control with time delay estimation. Mechatronics. 2013;23(3):310–317.

Murugan M, Ghoshal A, Bravo L, Xu F. Articulating axial-flow turbomachinery rotor blade for enabling variable speed gas turbine engine. Proceedings of the 2018 Joint Propulsion Conference; 2018 July. doi: 10.2514/6.2018-4522.

Xiaoguang L, Daohui Z, Xingang Z, Han J. Modeling and control of shape memory alloy actuator using feedback linearization. Proceedings of the 36th Chinese Control Conference; 2017. IEEE Xplore. p. 1222–1227.

Yi S, Ulsoy AG. Time-delayed vision-based DC motor control via rightmost eigenvalue assignment. Proceedings of the American Control Conference; 2014 July. p. 5564–5569. doi: 10.1109/ACC.2014.6858677.

List of Symbols, Abbreviations, and Acronyms

DC	direct current
FBL	feedback linearization
MRAC	Model Reference Adaptive Control
Ni	nickel
PC	personal computer
PID	proportional integral derivative
PV	proportional-velocity
SMA	Shape Memory Alloy
Ti	titanium

1 (PDF)	DEFENSE TECHNICAL INFORMATION CTR DTIC OCA
2 (PDF)	CCDC ARL IMAL HRA RECORDS MGMT FCDD RLD CL TECH LIB
1 (PDF)	GOVT PRINTG OFC A MALHOTRA
1 (PDF)	CCDC ARL FCDD RLV P M MURUGAN